Geophysical Research Letters

RESEARCH LETTER
10.1029/2021GL097472

Nocturnal Atmospheric Oxidative Processes in the Indo-Gangetic Plain and Their Variation During the COVID-19 Lockdowns

D. Meidan[1], S. S. Brown[2,3], V. Sinha[4], and Y. Rudich[1]

[1]Department of Earth and Planetary Sciences, Weizmann Institute of Science, Rehovot, Israel, [2]NOAA Chemical Sciences Laboratory, Boulder, CO, USA, [3]Department of Chemistry, University of Colorado, Boulder, CO, USA, [4]Department of Earth and Environmental Sciences, Indian Institute of Science Education and Research Mohali, Mohali, India

Key Points:

- Atmospheric response in the Indo-Gangetic Plain varied according to seasonal changes and emissions reductions due to COVID-19 lockdown
- NO_3 production was mainly affected by emission changes, while NO_3 sinks were sensitive to both emissions and seasonal changes
- Nitryl chloride, a photolytic chlorine radical source not previously considered in the inland Indo-Gangetic Plain, may be up to 5.5 ppbv

Supporting Information:

Supporting Information may be found in the online version of this article.

Correspondence to:

Y. Rudich,
yinon.rudich@weizmann.ac.il

Citation:

Meidan, D., Brown, S. S., Sinha, V., & Rudich, Y. (2022). Nocturnal atmospheric oxidative processes in the Indo-Gangetic Plain and their variation during the COVID-19 lockdowns. *Geophysical Research Letters*, *49*, e2021GL097472. https://doi.org/10.1029/2021GL097472

Received 11 JAN 2022
Accepted 28 MAR 2022

Author Contributions:

Conceptualization: D. Meidan, S. S. Brown, V. Sinha, Y. Rudich
Data curation: D. Meidan, V. Sinha
Formal analysis: D. Meidan, S. S. Brown
Funding acquisition: V. Sinha, Y. Rudich
Investigation: D. Meidan, S. S. Brown, V. Sinha, Y. Rudich
Methodology: D. Meidan, S. S. Brown, V. Sinha, Y. Rudich
Project Administration: Y. Rudich

Abstract This study investigates selected secondary atmospheric responses to the widely reported emission change attributed to COVID-19 lockdowns in the highly polluted Indo-Gangetic Plain (IGP) using ground-based measurements of trace gases and particulate matter. We used a chemical box-model to show that production of nighttime oxidant, NO_3, was affected mainly by emission decrease (average nighttime production rates 1.2, 0.8 and 1.5 ppbv hr^{-1} before, during and relaxation of lockdown restrictions, respectively), while NO_3 sinks were sensitive to both emission reduction and seasonal variations. We have also shown that the maximum potential mixing ratio of nitryl chloride, a photolytic chlorine radical source which has not been previously considered in the IGP, is as high as 5.5 ppbv at this inland site, resulting from strong nitrate radical production and a potentially large particulate chloride mass. This analysis suggests that air quality measurement campaigns and modeling explicitly consider heterogeneous nitrogen oxide and halogen chemistry.

Plain Language Summary The Indo-Gangetic Plain (IGP) is one of the most polluted regions on earth, with poor air quality affecting the majority of the Indian population. The atmospheric chemistry that transforms major regional emissions into harmful secondary pollutants is complex. Here, we quantify, for the first time, several important oxidative processes and show the potential for substantial oxidation of biogenic volatile organic compounds and the production of chlorine through unconventional chemistry in the IGP. We further show how these chemical cycles varied due to the emission reductions as a result of COVID-19 lockdown, findings that will serve to define their sensitivity to future emission changes in the region.

1. Introduction

Indo-Gangetic Plain (IGP) is home to almost half the Indian population. However, it accounts for only one fifth of India's land area, making it one of the most densely populated places on Earth. Known for its fertile lands, the IGP is a region with intense farming and agricultural activities. Due to the unique topography of the region, air pollution can either persist, a process relevant mostly during wintertime, or be impacted by long-range transport, which occurs mostly during the summer (pre-monsoon; Pawar et al., 2015). These factors result in frequent high-pollution events and rise in premature deaths related to poor air quality (David et al., 2019).

High concentrations of air pollutants in India and their impacts on the atmosphere and on human health have been extensively studied (Ghude et al., 2016; V. Kumar et al., 2016; Mohan & Saranya, 2019; Ojha et al., 2012; Yadav et al., 2014). Tropospheric ozone concentrations are influenced by the concentrations of ozone precursors (e.g., nitrogen oxides [$NO_x = NO + NO_2$] and volatile organic compounds), high exposure being detrimental to human health and agriculture (Y. Chen et al., 2021; Gaudel et al., 2018; Lefohn et al., 2018; Lu et al., 2020; Sharma et al., 2019; B. Sinha et al., 2015). Among the sources of anthropogenic emissions of NO_x and volatile organic compounds (VOCs) in the IGP region are industry, heavy traffic, power generation and agricultural biomass burning and residential fuel usage. Particulate matter smaller than 2.5 μm in diameter ($PM_{2.5}$) arises from primary emissions or forms in situ by secondary chemical reactions of gas-phase precursors such as NO_x, ozone, VOCs and sulfur dioxide (SO_2). 2016 World Health Organization (WHO) report (World Health, 2016) states that $PM_{2.5}$ levels in Delhi during the years 2011–2015 were the highest measured in mega-cities around the world and a large fraction of it (>50%) is derived from oxidation of precursors (Gani et al., 2019). More than 80% of Indian population suffers from poor air quality, with conditions deviating from WHO standards for $PM_{2.5}$ exposure. In the IGP, for example, $PM_{2.5}$ levels often exceed 160 μg/m^3 (Ravishankara et al., 2020). David et al. (2019) investigated

Resources: S. S. Brown, V. Sinha, Y. Rudich
Software: D. Meidan
Supervision: S. S. Brown, V. Sinha, Y. Rudich
Validation: S. S. Brown
Visualization: D. Meidan
Writing – original draft: D. Meidan
Writing – review & editing: D. Meidan, S. S. Brown, V. Sinha, Y. Rudich

impacts of emissions from different regions in India on premature death related to $PM_{2.5}$ exposure. They estimated that anthropogenic air pollution from the IGP region is responsible for 24%–31% of deaths in other regions in India, while about 70% of deaths are caused by local emissions.

Atmospheric oxidation capacity is controlled by concentrations and sources of the major oxidants OH, O_3 and NO_3. Chlorine radicals may also initiate tropospheric oxidation cycles, and recent observations in polluted regions have shown $ClNO_2$ to be an important photolytic precursor (Baker et al., 2016; Q. Chen et al., 2022; Haskins et al., 2019; Jeong et al., 2019; Wang et al., 2020; Xia et al., 2021). Nocturnal aqueous-phase reaction of particulate chloride with N_2O_5 produces $ClNO_2$ that affects next-day chemistry through photolysis (Osthoff et al., 2008). Sources of soluble chloride in the IGP include biomass burning, coal combustion, industrial waste incineration and to a lesser extent long-range transport of sea salt aerosol (Gunthe et al., 2021; Saiz-Lopez & von Glasow, 2012; Wang et al., 2019).

In order to limit the spread of COVID-19, governments imposed lockdowns in early 2020 that restricted mobility and public activities such as schools and businesses. India imposed a strict lockdown from the end of March until the beginning of May 2020. We studied a timeframe that can be regarded as three different periods: between 1 and 22 March 2020 (herein "before lockdown"), between 23 March–14 April 2020 (herein "strict lockdown"), and finally between 15 April–1 May 2020 (herein "lockdown relaxation"). The main differences between the two lockdown periods were that during lockdown relaxation, agricultural activities were approved (mainly harvesting) and some mobility restrictions were lifted (leading to slightly increased transportation emissions). Due to the lockdown, atmospheric concentrations of many anthropogenic pollutants, such as NO_x, anthropogenic VOC (AVOC) and SO_2, decreased. Forster et al. (2020) analyzed national mobility data and found an average decrease of >70% in mobility in India during the strict lockdown, resulting in NO_x emission decrease. Such sudden and unprecedented emission reductions present a unique opportunity to investigate chemical responses under different chemical scenarios.

In this study, we modeled the impact of lockdown restrictions on selected atmospheric oxidation pathways. These pathways are superimposed on changing seasonality of the chemical regime in winter-to-spring transition in the highly polluted IGP region. Elucidating NO_3 production and consumption pathways can help our understanding of the state of secondary atmospheric processes in the IGP under different atmospheric chemical regimes imposed by the lockdown.

2. Materials and Methods

2.1. Site Description

The measurement site is located on the outskirts of Mohali, a city in northwest IGP, in Indian state of Punjab. The measurement facility is housed in the Indian Institute of Science Education and Research (IISER; 30.667°N–76.729°E, 310 m a.s.l.) campus. The facility consists of a high sensitivity proton transfer reaction quadrupole mass spectrometer (PTR-QMS), an air quality station equipped with gas analyzers for the detection of trace levels (pptv–ppbv range) of O_3, NO_x, CO, SO_2, $PM_{2.5}$ and PM_{10} aerosol mass concentrations and a meteorological station for wind direction, wind speed, ambient temperature, relative humidity and solar radiation measurements (Met One Instruments Inc.). Inlets are located at 20 m above ground level. These instruments and their QA/QC have been comprehensively described in previous works reporting multi-year data from the facility (Chandra & Sinha, 2016; V. Kumar et al., 2020; V. Sinha et al., 2014). Calibrations performed before and after the lockdown were consistent with the general instrumental sensitivities and zero drifts. Overall uncertainty for all VOCs reported in this work was less than 20%, except for formaldehyde for which it was estimated to be less than 30% due to lack of calibration gas standard (see V. Kumar et al., 2020). For other trace gases and particulate matter (Pawar et al., 2015) it was less than 10%.

2.2. Model Description

The Framework for zero-Dimensional Atmospheric Modeling (F0AM), based on Master Chemical Mechanism (MCM) 3.3.1, was used to explore the effect of COVID-19 lockdown conditions on atmospheric oxidation processes associated with NO_3 (Jenkin et al., 2015; Wolfe et al., 2016). Observations of trace gases and particulates from the Mohali site were used to calculate the average diel cycles of species used to constrain the model in

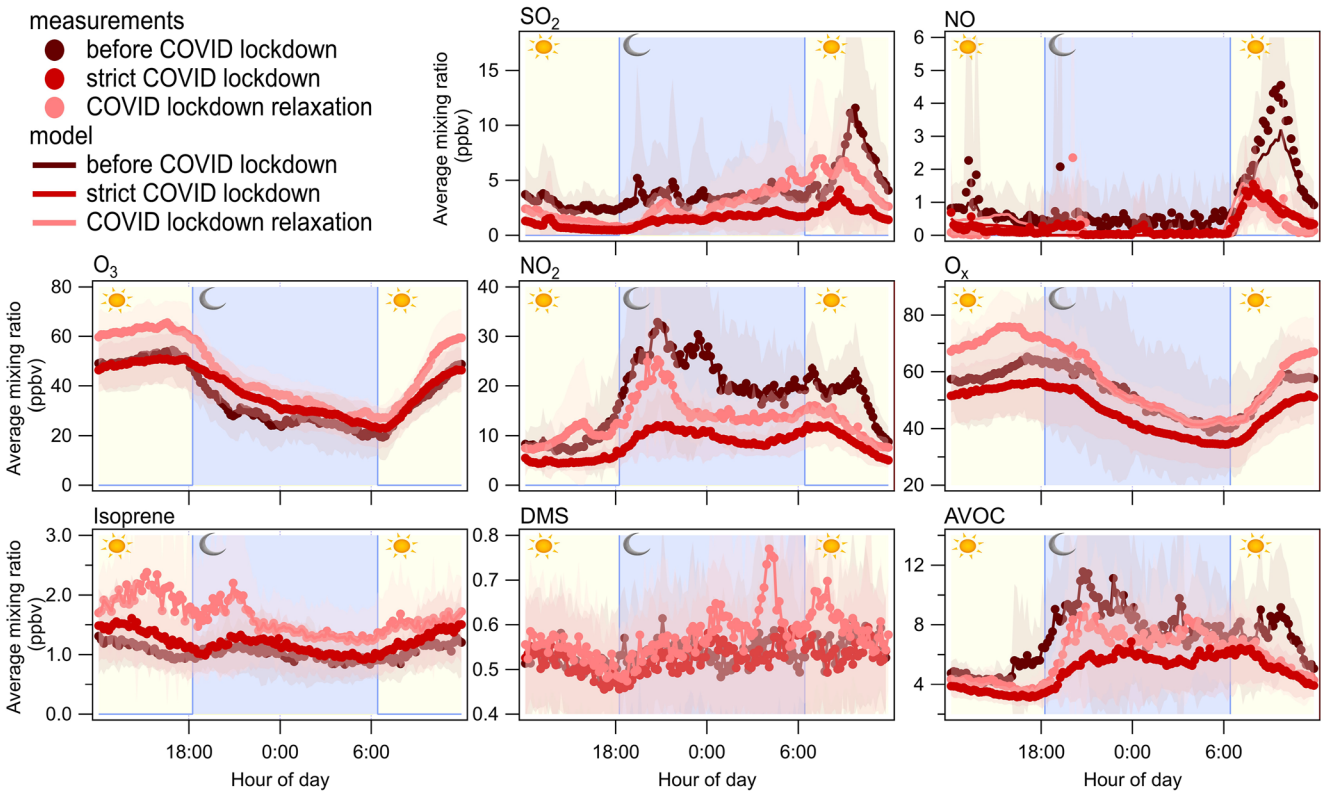

Figure 1. Diel cycles, at 10-min time resolution, of the three periods: before lockdown (brown), during strict lockdown (red), and during lockdown relaxation (pink). Dots represent measurements and solid lines represent simulation results. Shaded areas represent standard deviation of the measurements. Changes in isoprene and temperature between lockdown periods are driven by seasonality of the meteorology. During the lockdown, all pollutant mixing ratios decreased, except for ozone, which increased, especially during nighttime.

ten-minute time steps, same resolution as the model. The model was set to simulate a diel cycle with constrained ozone, NO_x, CO, SO_2, isoprene, DMS, 4 AVOCs, 11 aromatic VOCs, 6 oxygenated VOCs, relative humidity and temperature (Figure 1, Table S1 in Supporting Information S1, additional details on AVOC speciation can be found in Supporting Information S1). Photolysis rates were calculated in F0AM based on the trigonometric solar zenith angle function provided by the MCM. The method provides an upper limit of the photolysis rates since it does not account for surface albedo, overhead ozone column, cloud and aerosol extinction or enhancement, which may alter the photolysis rates (Wolfe et al., 2016). Modeled NO_x was constrained to the measurements, but partitioning between NO and NO_2 was allowed to vary.

In addition to the three lockdown periods (i.e., before lockdown, strict lockdown, and lockdown relaxation), approximately 17% of the before period measurements showed excess NO (>5 ppbv) and low ozone (<30 ppbv; Figure S1 in Supporting Information S1). These datapoints were treated as a separate category, since chemical evolution during events that end in full ozone titration differed considerably from that of non-titrated events (Figure S2 in Supporting Information S1) and are further explored in Supporting Information S1.

Average mixing ratios of measured species across 3 hours prior to sunset (15:30–18:30) provided the initial input for an atmospheric chemistry model intended to represent the residual layer. This approach mimics the transition from a well-mixed boundary layer to a two-layered nighttime boundary layer consisting of a surface layer (or nocturnal boundary layer), impacted by continuous emissions, and an overlying residual layer, consisting of late-afternoon chemical composition that is isolated from the surface emissions.

NO_3 is produced from reaction of NO_2 with ozone (Brown & Stutz, 2012) and is in equilibrium with its reservoir species N_2O_5, which undergoes heterogeneous uptake to form nitric acid (HNO_3) and $ClNO_2$. The first-order rate coefficient for N_2O_5 aerosol uptake is generally expressed as:

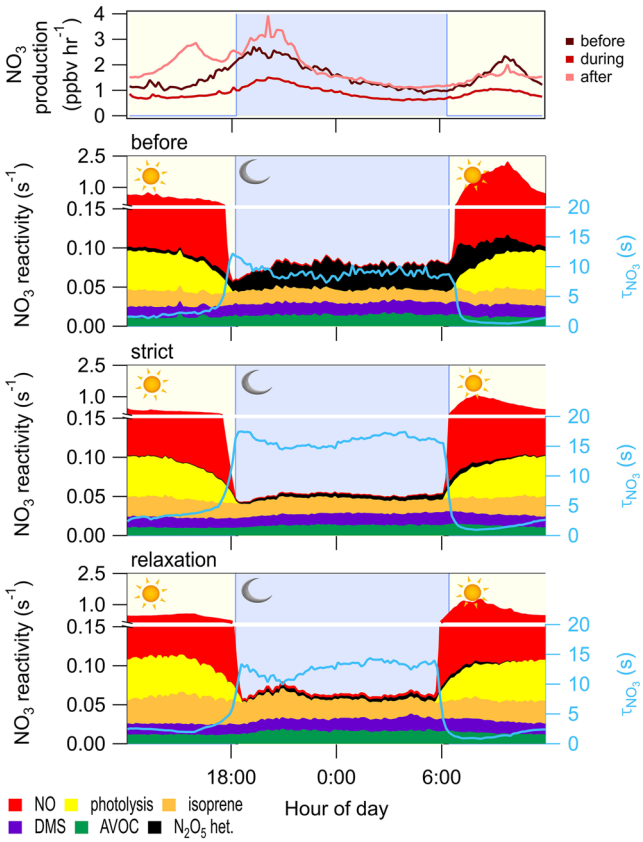

Figure 2. NO_3 production rate and reactivity toward anthropogenic volatile organic compound (AVOC), NO, isoprene, photolysis, heterogeneous uptake and DMS during the period before lockdown (top), during the strict lockdown (middle) and after relaxation of the lockdown (bottom). Cyan line is the modeled NO_3 lifetime. NO_3 has the shortest lifetime before the lockdown, when the overall emissions were higher. Reduction in aerosol surface area dramatically decreased heterogeneous loss of NO_3 and increased its atmospheric lifetime.

$$k_{\text{het. } N_2O_5} = \frac{\gamma \bar{c} SA}{4} \quad (1)$$

where, γ is the aerosol uptake coefficient, $\bar{c}$ the mean molecular speed of N_2O_5, and SA the aerosol surface area. N_2O_5 measurements that are used to constrain this parameter are not available at this site. Therefore, an uptake coefficient sensitivity test is described in details in Figure S3 of Supporting Information S1. The model uses a single representative uptake coefficient of $\gamma_{N_2O_5} = 10^{-2}$ (Chang et al., 2011; R. Kumar et al., 2014; McDuffie et al., 2018).

The first-order rate coefficient for the NO_3 loss through N_2O_5 aerosol uptake is then (Brown et al., 2003):

$$k_{\text{het. } NO_3} = K_{eq} [NO_2] k_{\text{het. } N_2O_5} \quad (2)$$

where, K_{eq} is the equilibrium constant between NO_2, NO_3 and N_2O_5.

Aerosol surface area was calculated from measured $PM_{2.5}$ and PM_{10} after assuming a typical size distribution in the IGP according to the relevant season and correction for hygroscopic growth (Pawar & Sinha, 2020). Figure S4 in Supporting Information S1 shows resultant surface area and calculated heterogeneous rate coefficients for NO_3 and N_2O_5.

3. Results

NO_3 is formed from the oxidation of NO_2 by ozone. It then reacts with NO_2 to establish an equilibrium with N_2O_5, which can act as a reservoir for NO_3 or as a loss pathway, by uptake onto aerosols. Since NO_3 is photolabile, it typically serves as an oxidant only during the night hours. Uptake of N_2O_5 to aerosols leads to HNO_3 and $ClNO_2$ production, with a yield that depends on the available chloride (Bertram & Thornton, 2009; Roberts et al., 2009). HNO_3 may partition to the aerosol phase as inorganic nitrate.

During daytime, reaction with NO and photolysis destroy NO_3 and recycle it to NO_x. The NO_3 production rate is calculated by:

$$P(NO_3) = k_{O_3+NO_2} [O_3] [NO_2] \quad (3)$$

During the strict lockdown, NO_x mixing ratios decreased and NO_3 production decreased correspondingly relative to before the lockdown. After the lockdown, a late evening NO_2 peak resulted in a NO_3 production peak, a feature that appeared only slightly in the prior periods.

Figure 2 shows NO_3 reactivity toward important atmospheric species and its modeled lifetime. NO_3 reactivity toward these species is calculated by:

$$k^{NO_3} = \sum k_i [X]_i \quad (4)$$

where, k_i is the rate coefficient ($cm^3\ s^{-1}$) for reaction between a species X of concentration $[X]_i$ and NO_3.

Steady-state lifetime, τ_{NO_3}, is given by the inverse of k^{NO_3} from Equations 2 and 4. Lifetime is normally calculated with observed NO_3. However, in the absence of such measurements at this site (or at any location in the IGP to date), (NO_3) in Equations 3 and 5 served as modeled concentration of NO_3:

$$[NO_3] = \tau_{NO_3} * P(NO_3) \quad (5)$$

where, P(NO_3) is the production rate of NO_3 (ppbv s^{-1}), as described in Equations 1 and 3.

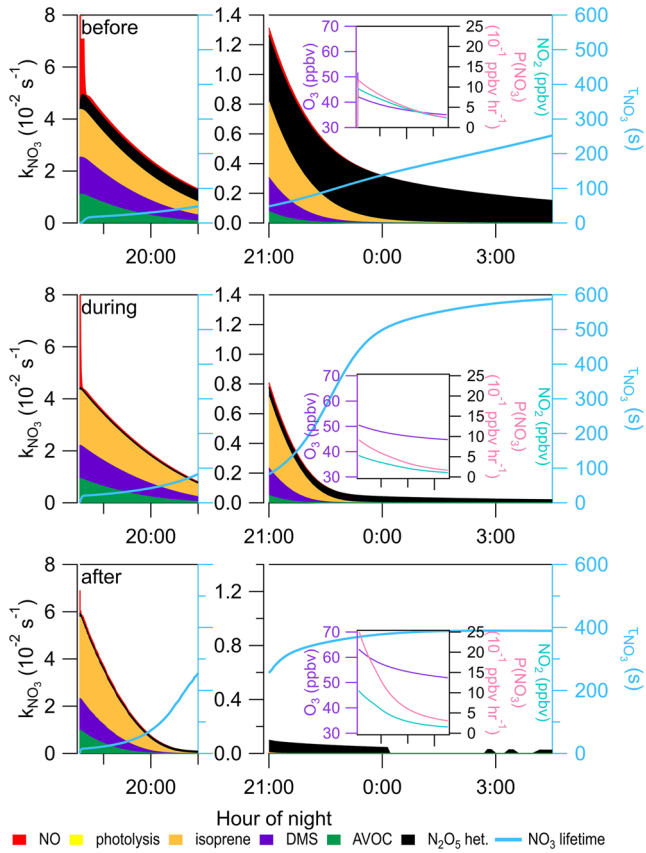

Figure 3. Nighttime NO_3 reactivity toward NO, isoprene, photolysis, heterogeneous uptake, DMS and anthropogenic volatile organic compound (AVOC) during the period before lockdown (top), during strict lockdown (middle) and after lockdown relaxation (bottom). Residual layer is split into the first (until 21:00, left plots) and second (from 21:00, right plots) part of the night to illustrate differences in reactivity scales. Ozone and NO_2 mixing ratios and production rate of NO_3 are shown in the inset for the full night period. Cyan line reflects NO_3 lifetime.

Production rate of nitrate radicals as shown in Equations 1 and 3 can be used as a useful metric for comparing the extent of nighttime chemistry in different megacities. For example, Brown et al. (2017) determined $P(NO_3)$ from measurements in a tower in the Asian megacity of Seoul, South Korea, in May to early June 2015. Median production rate in Seoul 2015 exceeded 90th percentile $P(NO_3)$ from nighttime research aircraft flights in a similar altitude range in Los Angeles, a comparably sized U.S. megacity. Figure S5 in Supporting Information S1 shows nighttime measurements from Seoul and Los Angeles with $P(NO_3)$ as calculated in our study. 10th percentile $P(NO_3)$ of all three studied periods in Mohali exceeded the 90th percentile production rate measured in Los Angeles. The lockdown relaxation period was measured during a similar time of year as the measurements made in Seoul and Los Angeles. However, median nighttime $P(NO_3)$ in Mohali were the largest during the 2020 lockdown relaxation period (1.5 ppbv hr^{-1}), compared to Seoul in 2015 (1.3 ppbv hr^{-1}) and Los Angeles in 2010 (0.3 ppbv hr^{-1}). These high NO_3 production rates are comparable to daytime chemical oxidation rates in polluted regions (Volkamer et al., 2010; Young et al., 2012) and lead to a significant nighttime oxidative capacity.

Figure 2 shows that diel profiles of NO_3 lifetime is similar in all periods. NO and sunlight are the main NO_3 daytime consumers, longest NO_3 lifetime occurs at sunset and shortest lifetime occurs at sunrise. Before the lockdown, nighttime NO_3 lifetime decreased rapidly (from ~12 s^{-1} to ~8 s^{-1} in under 3 hr) due to heterogeneous uptake by high loading of particulate matter. At the onset of the lockdown, significant decreases in particulate matter concentrations in the IGP region (Singh et al., 2020) eliminated this rapid loss of NO_3 by heterogeneous uptake, resulting in longer NO_3 lifetime. NO morning peak consumed most of the NO_3 (up to 90% Figure S6 in Supporting Information S1) during all periods. As the sun sets, NO mixing ratio decreased and the main NO_3 reactions are with isoprene, DMS and AVOC.

Figure S7 in Supporting Information S1 shows daytime ratio of NO_3 reactivity toward isoprene, DMS and AVOC to the overall NO_3 reactivity and predicted amount of produced NO_3 that reacted with isoprene, DMS and AVOC. Daytime NO_3 oxidation of these species increases from morning, and reached maximum daytime values in the afternoon. As seen in Figure 2, before the lockdown, NO_3 oxidation of these three species was approximately the same. However, upon strict lockdown, isoprene consumed more produced NO_3 during the day (0.08 ppbv hr^{-1}), and more than twofold after lockdown relaxation (0.25 ppbv hr^{-1}). Fuchs et al. (2017) and Williams et al. (2016) measured the reactivity of the main daytime oxidant, OH, in polluted areas in north China plain and megacity Beijing, respectively. They have found that during the daytime an average of ~10% of the OH reactivity is toward isoprene. This is comparable to 8%–10% NO_3 reactivity toward isoprene in the afternoon once lockdown is imposed.

Surface measurements at night are often not representative of chemistry within the entire boundary layer structure, which consists of both a nocturnal boundary layer and overlying residual layer. Following the approach of Baasandorj et al. (2017), the simulation of chemistry in the residual layer is initialized with atmospheric mixing ratios of the late afternoon, but the model of this layer remained isolated from further surface emissions. Figure 3 shows the calculated NO_3 reactivity, O_3 and NO_2 mixing ratios and modeled production rate of NO_3 predicted for the residual layer, which could not be directly sampled from this measurement site. Predicted production rate of NO_3 decreased as surface NO_2 (and, to a lesser extent, O_3) was consumed. O_3 mixing ratios in the residual layer increased between the three periods, likely as a result of seasonality in the photochemistry. NO_2 mixing ratios, by contrast, were impacted by COVID-19 lockdown, marked by a clear decrease. Consequently, during the strict lockdown, modeled NO_3 production rate was the slowest of the three periods, with fastest NO_3 production rates occurring upon lockdown relaxation, when O_3 mixing ratios were the highest.

While NO_3 in the surface and residual layers exhibits similar reactivity at the beginning of the night, predicted NO_3 lifetime in the residual layer increases as the residual layer VOCs are consumed in the absence of contact with surface-based emissions. Residual layer modeled reactivity of NO_3 toward NO is negligible, since NO is rapidly consumed by ozone within ~2–5 min. After the lockdown relaxation, isoprene mixing ratios rose due to higher temperatures and solar flux, as well as higher ozone mixing ratios. Therefore, consumption of the constituents in the residual layer was fastest after the lockdown relaxation. However, predicted NO_3 lifetime reached the highest values during the strict lockdown, when surface emissions and particulate matter loading were at their lowest.

Integrated production of NO_3 from NO_x over the course of one night in the residual layer exceeds initial mixing ratios of reactive VOCs such as DMS and isoprene, as discussed below. Therefore, loss of NO_3 and N_2O_5 transitions from NO_3 + VOC-dominated to heterogeneous uptake in the residual layer as reactive VOCs are consumed. This transition affects production of inorganic nitrate species HNO_3 and $ClNO_2$. Figure S8 in Supporting Information S1 shows a comparison of HNO_3 and $ClNO_2$ production potential in the residual and surface layers, here shown as the maximum $ClNO_2$ production using an assumed $ClNO_2$ yield, $\phi(ClNO_2) = 1$. In this simulation, $ClNO_2$ and HNO_3 are equal. Regardless of the assumed $ClNO_2$ yield, total amount of produced inorganic nitrate ($ClNO_2$ + HNO_3) would be equal to twice that of $ClNO_2$. Before the lockdown, nighttime maximum $ClNO_2$ production in the residual layer (3 ppbv) was about half that in the surface layer (5.5 ppbv). During the strict lockdown, maximum $ClNO_2$ production in both layers was similar (~1 ppbv). However, with the lifting of some lockdown restrictions, maximum $ClNO_2$ production in the residual layer exceeded production in the surface layer (2.5 and 1.5 ppbv, respectively) due to a faster N_2O_5 uptake rate.

VOC/NO_x ratios are a useful diagnostic for probing secondary pollutant formation regimes from both photochemistry and nighttime chemistry. The influence of this ratio on daytime ozone photochemistry is well established (Council, 1991; V. Kumar & Sinha, 2021; Seinfeld, 1989). During the day, this ratio indicates the competition between ozone production and consumption through photolysis of NO_2, oxidation of VOC, NO and NO_2 reaction with peroxy radicals, scavenging of ozone by NO etc. During the night, this ratio indicates the competition between NO_3- and O_3-dominant regimes of VOC oxidation. VOC/NO_x ratio also determines the competition between inorganic and organic nitrate production during the night and day. At low VOC/NO_x ratios, nighttime production of inorganic nitrate (HNO_3 and $ClNO_2$ from N_2O_5 uptake) increases while the level of organic nitrate (the major product of VOC oxidation by NO_3) decreases (Romer Present et al., 2020). The competition between inorganic nitrate and organic nitrate determines the aerosol yield and composition by changing the reaction pathways (Huang et al., 2021; Petit et al., 2021).

Using nighttime measurements from the residual layer in the southeast US, Edwards et al. (2017) calculated the transition between NO_3- and O_3-dominant regimes, which occurs at NO_x/isoprene ratio of approximately 0.5. Transition between inorganic and organic nitrate production occurs at NO_x/isoprene ratio of approximately 3. These transition points are shown in Figure 4, which also displays nighttime NO_x/VOC ratio in the simulation and in the measurements during the three studied periods. Before the lockdown, inorganic nitrate production was the main sink for NO_3. During the lockdown, nitrate production changed from inorganic- to organic-dominant, although the measurements rarely cross the line calculated by Edwards et al. (2017). In all three periods, NO_x/VOC ratio never reached the transition point to an O_3- (rather than NO_3) dominated nighttime chemistry (Edwards et al., 2017). Consequently, decreasing NO_x as occurred during the lockdown did not dramatically affect isoprene oxidation, which was always dominated by reactions with NO_3 (Figure S9 in Supporting Information S1). This also affected the maximum potential for $ClNO_2$ production (Figure S8 in Supporting Information S1), which decreased from nighttime maximum production of 5.5 ppbv before the lockdown to less than 1 ppbv during the strict lockdown, followed by an increase to 1.5 ppbv upon lockdown relaxation. This maximum $ClNO_2$ production changes have the capability to affect photochemistry and next-day ozone production, however, this depends on available chloride. Gunthe et al. (2021) measured chemical composition of PM_1 in Delhi and found that during episodes with high chloride, its concentration in PM_1 may reach 22.1 ± 13.7 μg m^{-3} (equivalent to 15 ± 9 ppbv), whereas during the entire period, measured chloride was 5.9 ± 9.1 μg m^{-3} (equivalent to 4 ± 6 ppbv). Gani et al. (2019) also measured the chemical composition of PM_1 in Delhi and found that diel cycle of chloride in PM_1 has a morning peak of up to 50 μg m^{-3} (equivalent to 33 ppbv) during winter. Nighttime winter concentrations of chloride in PM_1 varied between 20 and 30 μg m^{-3} (equivalent to 13–20 ppbv). Reaching such concentrations in an inland location such as the IGP indicates there is sufficient chloride to sustain the maximum potential for

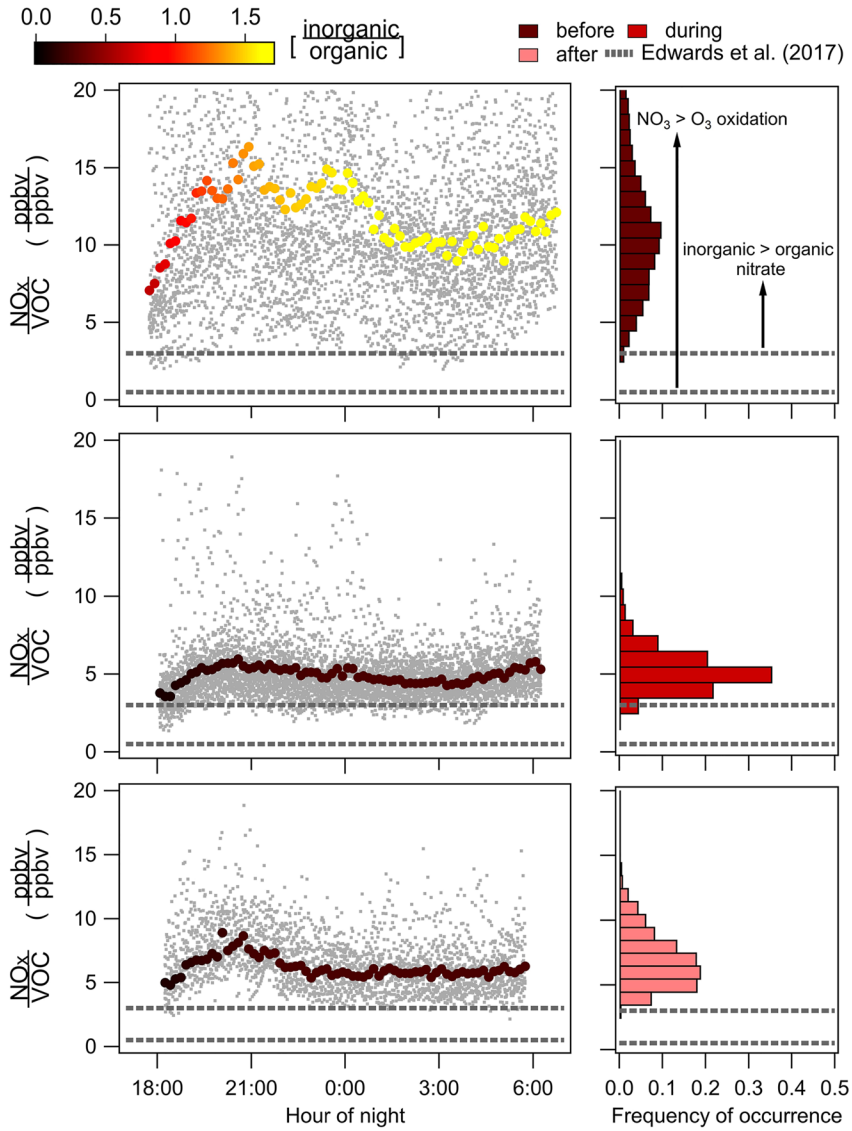

Figure 4. Left—NO_x/volatile organic compound (VOC) ratio during nighttime from the model. Color scale shows the ratio between inorganic and organic nitrate production. Gray dots reflect the spread of measured data during the night. Right—NO_x/VOC ratio histograms of measured nighttime data. Data is shown for the three periods studied: before COVID-19 lockdown (top), during strict lockdown (middle) and after lockdown relaxation (bottom). Dashed gray lines are the transition points modeled by Edwards et al. (2017) (0.5 - NO_3-to-O_3 dominant regime; 3 - inorganic-to-organic-nitrate-production dominant regime) as is shown in the upper right panel.

$ClNO_2$ production in the region. Therefore, calculated maximum $ClNO_2$ production may be close to actual levels, and this potential chlorine chemistry requires further investigation in the IGP.

4. Conclusions

Effects of emission reductions during COVID-19 lockdowns on atmospheric composition and air quality have been studied in many places around the world and will continue to be of scientific and public interest for years to come. Lockdown emissions reductions combined with seasonal variations provide a unique opportunity to investigate selected oxidation processes at a site in the Indo-Gangetic Plain, a highly polluted region, where nighttime oxidation has rarely, if ever, been investigated. Our work quantifies, for the first time in India, rates of several atmospheric oxidation processes. These processes include the consumption of VOCs by NO_3 radicals, and potential production of $ClNO_2$. These processes were affected differently by changes related to the transition from

winter to spring and to emission changes due to COVID-19 pandemic. Nighttime chemistry was highly influenced by reduction in emissions related to COVID-19 restrictions. During the lockdown, nighttime NO_3 average production rates and $ClNO_2$ production decreased by 50% and 80%, respectively, accompanied by a clear shift in nitrate production from an inorganic- to an organic-nitrate-production-dominant regime.

Extreme pollution levels associated with the IGP lead to increased rates of unconventional atmospheric chemistry processes, such as those investigated here. This manuscript identifies several processes that have not been studied in this region previously and were likely modified by pollutant emission changes during COVID-19 lockdowns. Future work to quantify these processes, their contribution to particulate matter and ozone chemistry in the IGP and their dependence on emissions will be of substantial interest to the air quality scientific and policy communities.

Data Availability Statement

The observational data used for this study is available online at https://data.mendeley.com/datasets/svvf9nwc43/draft?a=5ba5e802-386f-410b-b46f-8107d67f6158.

Acknowledgments
We acknowledge the Indian Institute of Science Education and Research Mohali Atmospheric Chemistry Facility for data and University Grant Commission (UGC) India and Israel Science Foundation (ISF), Israel for funding the project. We thank Baerbel Sinha, Vidit Parkar and Abhishek Mishra for technical assistance. This work was funded by a joint ISF and UGC of India Research Grant (# 2727/17 and F. No. 6-4/2018(IC)). This work was supported by a research grant from the Weizmann Institute sustainability and energy research initiative.

References

Baasandorj, M., Hoch, S. W., Bares, R., Lin, J. C., Brown, S. S., Millet, D. B., et al. (2017). Coupling between chemical and meteorological processes under persistent cold-air pool conditions: Evolution of wintertime PM2.5 pollution events and N_2O_5 observations in Utah's Salt Lake Valley. *Environmental Science & Technology*, *51*(11), 5941–5950. https://doi.org/10.1021/acs.est.6b06603

Baker, A. K., Sauvage, C., Thorenz, U. R., van Velthoven, P., Oram, D. E., Zahn, A., et al. (2016). Evidence for strong, widespread chlorine radical chemistry associated with pollution outflow from continental Asia. *Scientific Reports*, *6*(1), 36821. https://doi.org/10.1038/srep36821

Bertram, T. H., & Thornton, J. A. (2009). Toward a general parameterization of N_2O_5 reactivity on aqueous particles: The competing effects of particle liquid water, nitrate and chloride. *Atmospheric Chemistry and Physics*, *9*(21), 8351–8363. https://doi.org/10.5194/acp-9-8351-2009

Brown, S. S., An, H., Lee, M., Park, J.-H., Lee, S.-D., Fibiger, D. L., et al. (2017). Cavity enhanced spectroscopy for measurement of nitrogen oxides in the Anthropocene: Results from the Seoul tower during MAPS 2015. *Faraday Discussions*, *200*(0), 529–557. https://doi.org/10.1039/c7fd00001d

Brown, S. S., Stark, H., & Ravishankara, A. R. (2003). Applicability of the steady state approximation to the interpretation of atmospheric observations of NO_3 and N_2O_5. *Journal of Geophysical Research*, *108*(D17), 4539. https://doi.org/10.1029/2003jd003407

Brown, S. S., & Stutz, J. (2012). Nighttime radical observations and chemistry. *Chemical Society Reviews*, *41*(19), 6405–6447. https://doi.org/10.1039/c2cs35181a

Chandra, B. P., & Sinha, V. (2016). Contribution of post-harvest agricultural paddy residue fires in the N.W. Indo-Gangetic Plain to ambient carcinogenic benzenoids, toxic isocyanic acid and carbon monoxide. *Environment International*, *88*, 187–197. https://doi.org/10.1016/j.envint.2015.12.025

Chang, W. L., Bhave, P. V., Brown, S. S., Riemer, N., Stutz, J., & Dabdub, D. (2011). Heterogeneous atmospheric chemistry, ambient measurements, and model calculations of N_2O_5: A review. *Aerosol Science and Technology*, *45*(6), 665–695. https://doi.org/10.1080/02786826.2010.551672

Chen, Q., Xia, M., Peng, X., Yu, C., Sun, P., Li, Y., et al. (2022). Large daytime molecular chlorine missing source at a suburban site in East China. *Journal of Geophysical Research: Atmospheres*, *127*(4), e2021JD035796. https://doi.org/10.1029/2021JD035796

Chen, Y., Beig, G., Archer-Nicholls, S., Drysdale, W., Acton, W. J. F., Lowe, D., et al. (2021). *Avoiding high ozone pollution in Delhi, India*. Faraday Discussions.

Council, N. R. (1991). *Rethinking the ozone problem in urban and regional air pollution* (p. 524). The National Academies Press.

David, L. M., Ravishankara, A. R., Kodros, J. K., Pierce, J. R., Venkataraman, C., & Sadavarte, P. (2019). Premature mortality due to PM2.5 over India: Effect of atmospheric transport and anthropogenic emissions. *GeoHealth*, *3*(1), 2–10. https://doi.org/10.1029/2018gh000169

Edwards, P. M., Aikin, K. C., Dube, W. P., Fry, J. L., Gilman, J. B., De Gouw, J. A., et al. (2017). Transition from high- to low-NO_x control of night-time oxidation in the southeastern US. *Nature Geoscience*, *10*, 490. https://doi.org/10.1038/ngeo2976

Forster, P. M., Forster, H. I., Evans, M. J., Gidden, M. J., Jones, C. D., Keller, C. A., et al. (2020). Current and future global climate impacts resulting from COVID-19. *Nature Climate Change*, *10*(10), 913–919. https://doi.org/10.1038/s41558-020-0883-0

Fuchs, H., Tan, Z., Lu, K., Bohn, B., Broch, S., Brown, S. S., et al. (2017). OH reactivity at a rural site (Wangdu) in the north China plain: Contributions from OH reactants and experimental OH budget. *Atmospheric Chemistry and Physics*, *17*(1), 645–661. https://doi.org/10.5194/acp-17-645-2017

Gani, S., Bhandari, S., Seraj, S., Wang, D. S., Patel, K., Soni, P., et al. (2019). Submicron aerosol composition in the world's most polluted megacity: The Delhi Aerosol Supersite study. *Atmospheric Chemistry and Physics*, *19*(10), 6843–6859. https://doi.org/10.5194/acp-19-6843-2019

Gaudel, A., Cooper, O. R., Ancellet, G., Barret, B., Boynard, A., Burrows, J. P., et al. (2018). Tropospheric Ozone Assessment Report: Present-day distribution and trends of tropospheric ozone relevant to climate and global atmospheric chemistry model evaluation. *Elementa: Science of the Anthropocene*, *6*, 39. https://doi.org/10.1525/elementa.291

Ghude, S. D., Chate, D. M., Jena, C., Beig, G., Kumar, R., Barth, M. C., et al. (2016). Premature mortality in India due to PM2.5 and ozone exposure. *Geophysical Research Letters*, *43*(9), 4650–4658. https://doi.org/10.1002/2016gl068949

Gunthe, S. S., Liu, P., Panda, U., Raj, S. S., Sharma, A., Darbyshire, E., et al. (2021). Enhanced aerosol particle growth sustained by high continental chlorine emission in India. *Nature Geoscience*, *14*(2), 77–84. https://doi.org/10.1038/s41561-020-00677-x

Haskins, J. D., Lopez-Hilfiker, F. D., Lee, B. H., Shah, V., Wolfe, G. M., DiGangi, J., et al. (2019). Anthropogenic control over wintertime oxidation of atmospheric pollutants. *Geophysical Research Letters*, *46*(24), 14826–14835. https://doi.org/10.1029/2019GL085498

Huang, W., Yang, Y., Wang, Y., Gao, W., Li, H., Zhang, Y., et al. (2021). Exploring the inorganic and organic nitrate aerosol formation regimes at a suburban site on the North China Plain. *The Science of the Total Environment*, *768*, 144538. https://doi.org/10.1016/j.scitotenv.2020.144538

Jenkin, M. E., Young, J. C., & Rickard, A. R. (2015). The MCM v3.3.1 degradation scheme for isoprene. *Atmospheric Chemistry and Physics*, *15*(20), 11433–11459. https://doi.org/10.5194/acp-15-11433-2015

Jeong, D., Seco, R., Gu, D., Lee, Y., Nault, B. A., Knote, C. J., et al. (2019). Integration of airborne and ground observations of nitryl chloride in the Seoul metropolitan area and the implications on regional oxidation capacity during KORUS-AQ 2016. *Atmospheric Chemistry and Physics*, *19*(19), 12779–12795. https://doi.org/10.5194/acp-19-12779-2019

Kumar, R., Barth, M. C., Madronich, S., Naja, M., Carmichael, G. R., Pfister, G. G., et al. (2014). Effects of dust aerosols on tropospheric chemistry during a typical pre-monsoon season dust storm in northern India. *Atmospheric Chemistry and Physics*, *14*(13), 6813–6834. https://doi.org/10.5194/acp-14-6813-2014

Kumar, V., Beirle, S., Dörner, S., Mishra, A. K., Donner, S., Wang, Y., et al. (2020). Long-term MAX-DOAS measurements of NO_2, HCHO, and aerosols and evaluation of corresponding satellite data products over Mohali in the Indo-Gangetic Plain. *Atmospheric Chemistry and Physics*, *20*(22), 14183–14235. https://doi.org/10.5194/acp-20-14183-2020

Kumar, V., Sarkar, C., & Sinha, V. (2016). Influence of post-harvest crop residue fires on surface ozone mixing ratios in the N.W. IGP analyzed using 2 years of continuous in situ trace gas measurements. *Journal of Geophysical Research: Atmospheres*, *121*(7), 3619–3633. https://doi.org/10.1002/2015jd024308

Kumar, V., & Sinha, V. (2021). Season-wise analyses of VOCs, hydroxyl radicals and ozone formation chemistry over north-west India reveal isoprene and acetaldehyde as the most potent ozone precursors throughout the year. *Chemosphere*, 131184. https://doi.org/10.1016/j.chemosphere.2021.131184

Lefohn, A. S., Malley, C. S., Smith, L., Wells, B., Hazucha, M., Simon, H., et al. (2018). Tropospheric ozone assessment report: Global ozone metrics for climate change, human health, and crop/ecosystem research. *Elementa: Science of the Anthropocene*, *6*, 27. https://doi.org/10.1525/elementa.279

Lu, X., Zhang, L., Wang, X., Gao, M., Li, K., Zhang, Y., et al. (2020). Rapid increases in warm-season surface ozone and resulting health impact in China since 2013. *Environmental Science and Technology Letters*, *7*(4), 240–247. https://doi.org/10.1021/acs.estlett.0c00171

McDuffie, E. E., Fibiger, D. L., Dubé, W. P., Lopez-Hilfiker, F., Lee, B. H., Thornton, J. A., et al. (2018). Heterogeneous N_2O_5 uptake during winter: Aircraft measurements during the 2015 WINTER campaign and critical evaluation of current parameterizations. *Journal of Geophysical Research: Atmospheres*, *123*(8), 4345–4372. https://doi.org/10.1002/2018jd028336

Mohan, S., & Saranya, P. (2019). Assessment of tropospheric ozone at an industrial site of Chennai megacity. *Journal of the Air & Waste Management Association*, *69*(9), 1079–1095. https://doi.org/10.1080/10962247.2019.1604451

Ojha, N., Naja, M., Singh, K. P., Sarangi, T., Kumar, R., Lal, S., et al. (2012). Variabilities in ozone at a semi-urban site in the Indo-Gangetic Plain region: Association with the meteorology and regional processes. *Journal of Geophysical Research*, *117*(D20), D20301. https://doi.org/10.1029/2012jd017716

Osthoff, H. D., Roberts, J. M., Ravishankara, A. R., Williams, E. J., Lerner, B. M., Sommariva, R., et al. (2008). High levels of nitryl chloride in the polluted subtropical marine boundary layer. *Nature Geoscience*, *1*(5), 324–328. https://doi.org/10.1038/ngeo177

Pawar, H., Garg, S., Kumar, V., Sachan, H., Arya, R., Sarkar, C., et al. (2015). Quantifying the contribution of long-range transport to particulate matter (PM) mass loadings at a suburban site in the North-Western Indo-Gangetic Plain (NW-IGP). *Atmospheric Chemistry and Physics*, *15*(16), 9501–9520. https://doi.org/10.5194/acp-15-9501-2015

Pawar, H., & Sinha, B. (2020). Humidity, density, and inlet aspiration efficiency correction improve accuracy of a low-cost sensor during field calibration at a suburban site in the North-Western Indo-Gangetic plain (NW-IGP). *Aerosol Science and Technology*, *54*(6), 685–703. https://doi.org/10.1080/02786826.2020.1719971

Petit, J. E., Dupont, J. C., Favez, O., Gros, V., Zhang, Y., Sciare, J., et al. (2021). Response of atmospheric composition to COVID-19 lockdown measures during spring in the Paris region (France). *Atmospheric Chemistry and Physics Discussions*, *2021*, 1–24. https://doi.org/10.5194/acp-21-17167-2021

Ravishankara, A. R., David, L. M., Pierce, J. R., & Venkataraman, C. (2020). Outdoor air pollution in India is not only an urban problem. *Proceedings of the National Academy of Sciences*, *117*(46), 28640–28644. https://doi.org/10.1073/pnas.2007236117

Roberts, J. M., Osthoff, H. D., Brown, S. S., Ravishankara, A. R., Coffman, D., Quinn, P., & Bates, T. (2009). Laboratory studies of products of N_2O_5 uptake on Cl^- containing substrates. *Geophysical Research Letters*, *36*(20), L20808. https://doi.org/10.1029/2009gl040448

Romer Present, P. S., Zare, A., & Cohen, R. C. (2020). The changing role of organic nitrates in the removal and transport of NOx. *Atmospheric Chemistry and Physics*, *20*(1), 267–279. https://doi.org/10.5194/acp-20-267-2020

Saiz-Lopez, A., & von Glasow, R. (2012). Reactive halogen chemistry in the troposphere. *Chemical Society Reviews*, *41*(19), 6448–6472. https://doi.org/10.1039/c2cs35208g

Seinfeld, J. H. (1989). Urban air pollution: State of the science. *Science*, *243*(4892), 745–752. https://doi.org/10.1126/science.243.4892.745

Sharma, A., Ojha, N., Pozzer, A., Beig, G., & Gunthe, S. S. (2019). Revisiting the crop yield loss in India attributable to ozone. *Atmospheric Environment X*, *1*, 100008. https://doi.org/10.1016/j.aeaoa.2019.100008

Singh, V., Singh, S., Biswal, A., Kesarkar, A. P., Mor, S., & Ravindra, K. (2020). Diurnal and temporal changes in air pollution during COVID-19 strict lockdown over different regions of India. *Environmental Pollution*, *266*, 115368. https://doi.org/10.1016/j.envpol.2020.115368

Sinha, B., Singh Sangwan, K., Maurya, Y., Kumar, V., Sarkar, C., Chandra, B. P., & Sinha, V. (2015). Assessment of crop yield losses in Punjab and Haryana using 2 years of continuous in situ ozone measurements. *Atmospheric Chemistry and Physics*, *15*(16), 9555–9576. https://doi.org/10.5194/acp-15-9555-2015

Sinha, V., Kumar, V., & Sarkar, C. (2014). Chemical composition of pre-monsoon air in the Indo-Gangetic Plain measured using a new air quality facility and PTR-MS: High surface ozone and strong influence of biomass burning. *Atmospheric Chemistry and Physics*, *14*(12), 5921–5941. https://doi.org/10.5194/acp-14-5921-2014

Volkamer, R., Sheehy, P., Molina, L. T., & Molina, M. J. (2010). Oxidative capacity of the Mexico City atmosphere—Part 1: A radical source perspective. *Atmospheric Chemistry and Physics*, *10*(14), 6969–6991. https://doi.org/10.5194/acp-10-6969-2010

Wang, X., Jacob, D. J., Eastham, S. D., Sulprizio, M. P., Zhu, L., Chen, Q., et al. (2019). The role of chlorine in global tropospheric chemistry. *Atmospheric Chemistry and Physics*, *19*(6), 3981–4003. https://doi.org/10.5194/acp-19-3981-2019

Wang, X., Jacob, D. J., Fu, X., Wang, T., Breton, M. L., Hallquist, M., et al. (2020). Effects of anthropogenic chlorine on PM2.5 and ozone air quality in China. *Environmental Science & Technology*, *54*(16), 9908–9916. https://doi.org/10.1021/acs.est.0c02296

Williams, J., Keßel, S. U., Nölscher, A. C., Yang, Y., Lee, Y., Yáñez-Serrano, A. M., et al. (2016). Opposite OH reactivity and ozone cycles in the Amazon rainforest and megacity Beijing: Subversion of biospheric oxidant control by anthropogenic emissions. *Atmospheric Environment*, *125*(1), 112–118. https://doi.org/10.1016/j.atmosenv.2015.11.007

Wolfe, G. M., Marvin, M. R., Roberts, S. J., Travis, K. R., & Liao, J. (2016). The Framework for 0-D atmospheric modeling (F0AM) v3.1. *Geoscientific Model Development*, *9*(9), 3309–3319. https://doi.org/10.5194/gmd-9-3309-2016

World Health, O. (2016). *Ambient air pollution: A global assessment of exposure and burden of disease*. World Health Organization.

Xia, M., Peng, X., Wang, W., Yu, C., Wang, Z., Tham, Y. J., et al. (2021). Winter $ClNO_2$ formation in the region of fresh anthropogenic emissions: Seasonal variability and insights into daytime peaks in northern China. *Atmospheric Chemistry and Physics*, *21*(20), 15985–16000. https://doi.org/10.5194/acp-21-15985-2021

Yadav, R., Sahu, L. K., Jaaffrey, S. N. A., & Beig, G. (2014). Distributions of ozone and related trace gases at an urban site in Western India. *Journal of Atmospheric Chemistry*, *71*(2), 125–144. https://doi.org/10.1007/s10874-014-9286-9

Young, C. J., Washenfelder, R. A., Roberts, J. M., Mielke, L. H., Osthoff, H. D., Tsai, C., et al. (2012). Vertically resolved measurements of nighttime radical reservoirs in Los Angeles and their contribution to the urban radical budget. *Environmental Science & Technology*, *46*(20), 10965–10973. https://doi.org/10.1021/es302206a

References From the Supporting Information

Brown, S. S., An, H., Lee, M., Park, J.-H., Lee, S.-D., Fibiger, D. L., et al. (2017). Cavity enhanced spectroscopy for measurement of nitrogen oxides in the Anthropocene: Results from the Seoul tower during MAPS 2015. *Faraday Discussions*, *200*(0), 529–559. https://doi.org/10.1039/C7FD00001D

McDuffie, E. E., Fibiger, D. L., Dubé, W. P., Lopez-Hilfiker, F., Lee, B. H., Thornton, J. A., et al. (2018). Heterogeneous N_2O_5 uptake during winter: Aircraft measurements during the 2015 WINTER campaign and critical evaluation of current parameterizations. *Journal of Geophysical Research: Atmospheres*, *123*(8), 4345–4372. https://doi.org/10.1002/2018JD028336

Yu, C., Wang, Z., Xia, M., Fu, X., Wang, W., Tham, Y. J., et al. (2020). Heterogeneous N_2O_5 reactions on atmospheric aerosols at four Chinese sites: Improving model representation of uptake parameters. *Atmospheric Chemistry and Physics*, *20*(7), 4367–4378. https://doi.org/10.5194/acp-20-4367-2020